Pergamon

PII: S0277-5387(97)00047-8

Polyhedron Vol. 16, No. 18, pp. 3197–3211, 1997

0277-5387/97 $17.00+0.00

Desulfurization, deoxygenation and denitrogenation of heterocycles by a palladium surface: a mechanistic study of thiophene, furan and pyrrole on Pd(111) using laser-induced thermal desorption with Fourier-transform mass spectrometry

Tracy E. Caldwell and Donald P. Land*

Department of Chemistry, University of California, Davis, CA 95616, U.S.A.

Abstract—The following contains a review of recent work, plus new results, from our laboratory using laser-induced thermal desorption with Fourier transform mass spectrometry (LITD/FTMS) to elucidate the decomposition mechanism of thiophene, furan and pyrrole on Pd(111). The results show that all three heterocycles react differently on Pd, despite their similarity in structure. Thiophene decomposes at 300 K *via* a C_4H_4 intermediate species, which subsequently hydrogenates and desorbs as 1,3-butadiene. The cleavage between the C—S bonds of thiophene results in the deposition of sulfur, which remains on the Pd(111) surface. In direct contrast to thiophene, furan decomposition on Pd(111) is shown to proceed at 300 K *via* elimination of α-H and CO, leaving a C_3H_3 species on the surface. Heating to 350 K causes dimerization of the C_3 species, forming benzene. In this case, oxygen is removed efficiently from the Pd(111) surface. Preliminary results of pyrrole on Pd(111) indicate that decomposition occurs at around 230 K, a lower temperature than either thiophene or furan. The only reaction product observed is HCN. The data cannot be readily explained by a pathway involving either a C_4 or a C_3 species, however, our results indicate the presence of some hydrocarbon species that decomposes above 325 K yielding hydrogen and above 500 K to give HCN. Removal of nitrogen from Pd(111) is similar to that of furan, in that the formation and subsequent desorption of HCN removes a significant fraction of nitrogen from the surface. © 1997 Elsevier Science Ltd

Keywords: desulfurization; deoxygenation; denitrogenation; laser-desorption; mass spectrometry; thiophene; furan; pyrrole; palladium.

INTRODUCTION

The world's reserve of crude oil is limited and non-renewable and the amount we have at hand is not accurately known [1]. Motivated by this and other environmental concerns, petroleum and petrochemical industries are considering other carbon sources as feed stock material for the production of fuels, which include heavy crudes and residua, coal and biomass resources. Yet the presence of organosulfur, -oxygen and -nitrogen compounds have plagued these alternative feed stocks by ultimately degrading the quality of fuels and reducing the efficiency at which they are produced [2]. The deleterious effects of these heteroatoms (S, O and N), in such things as corrosion of engine parts, NO_x and SO_x emissions, as well as the deactivation of refinement catalysts, have made the removal of these species an issue of importance. The current methods, however, are costly, both financially and energetically and the steps taken to improve the process (i.e. through the development of new catalysts and the modification of those already in existence) are achieved mostly through trial and error.

Recently, those industries relying on catalysis have recognized the need for a fundamental, molecular understanding of the working catalyst surface. Fundamental issues important to all heterogeneous chemistry include the relationship between surface structure and surface reactivity, as well as the competition

* Author to whom correspondence should be addressed.

between C—C, C—H and C—X (X = S, O and N) bond formation and cleavage catalyzed by transition metal surfaces. By exploring molecular structure and mechanisms, in addition to characterizing the active surface, studies such as those presented here can provide a basis for the rational design and modification of catalyst activity and selectivity.

Thiophenes are among the most common forms of sulfur-containing species found naturally in crude oil [3–5]. Oxygenated compounds are the most prevalent hetero-compounds in liquids derived from coal and biomass, with furanic rings among the most important of these [6,7]. Nitrogenated compounds, like pyrrole, are also common in coal-derived liquids and shale oil, however, their presence is most problematic in synthetic feed stocks and heavier petroleum fractions, where nitrogen concentrations are higher than those found in lighter petroleum feeds [8–11]. Due to their prevalence and aromatic stability, heterocompounds like thiophene, furan and pyrrole are used most often as models for understanding the interactions between these types of species and the catalytic surface. The same catalysts are used for all three classes of compounds and typically consist of alumina-supported sulfides of Mo or W [7]. The addition of a late transition metal, such as Co or Ni, as a promoter has been reported to increase catalytic activity by about an order of magnitude [12]; however, little is known about the surface chemistry of heterocycles on late transition metals and even less is understood about the effects of Pd, in particular. Our results show that, despite the industry standard of treating all heterocompounds under the same conditions, furan, thiophene and pyrrole react strikingly differently on Pd(111). We also shed some light on the question of the relative order of hydrogenation and ring opening.

The following contains a compilation of the initial results on the products and mechanisms of the individual, low-temperature decompositions of thiophene, furan and pyrrole on clean Pd(111) under UHV conditions using laser-induced thermal desorption with Fourier transform mass spectrometry (LITD/FTMS). The reactivity of these three systems are compared on the Pd(111) surface and are found to behave quite differently, despite the similarities in their structure. This work also supports conclusions drawn by previous investigators, using other metals, in which a metallocycle intermediate is proposed for the decomposition of thiophene [13–17], however, our results for furan on Pd(111) are rather unexpected compared with what was observed for furan on Mo foils [18], Cu(110) [19], Ag(110) [20] and O/Ag(110) [21]. The preliminary results of pyrrole decomposition on Pd(111) are discussed and related to pyrrole on Ni(100) [22], Rh(111) [23], O/Mo(100) [24], Pt(111) [25], Cu(110) [19] and Fe_2O_3 [26].

Laser-induced thermal desorption/Fourier transform mass spectrometry (LITD/FTMS) has been developed as one of the most sensitive probes to yield time dependent molecular information from surfaces [27]. This technique produces a "snapshot" of the molecular composition of an adsorbate layer with sub-second time resolution and does so for samples ranging from bulk solids, to thin layers, to coverages of less than one sample molecule for every 10,000 surface atoms (250 femtomol cm^{-1} [28]. This makes LITD/FTMS an ideal tool for analyzing the complex mixtures present on a variety of surfaces. The prompt, pulsed-laser-induced desorption of surface-bound species can provide information on the kinetics of adsorption and desorption, on surface diffusion and on the kinetics and mechanisms of adsorbed-species reactions [29,30].

LITD uses a focused, pulsed laser beam to generate a thermal spike (800 K in 8 ns) over a 1 mm diameter spot on a surface. This phenomenal heating rate (10^{11} K s^{-1}) can access high-energy reaction pathways and typically results in desorption of species adsorbed under the laser beam before they have a chance to react [29,31,32]. Many species which would react on the surface under slow heating conditions can be desorbed intact under rapid laser heating. This is because direct desorption is entropically more favorable and can dominate in the high-temperature reaction regime accessed by laser heating. LITD, then, results in a short (μs) burst of material desorbing from the surface which one wishes to analyze. FTMS is an ideal technique for this, because the technique is inherently pulsed and results in a complete (10–800 Dalton typical), high-resolution mass spectrum [33–36] for each single laser pulse [27,28,37].

EXPERIMENTAL

The experiments are performed in an ultra-high vacuum chamber (10^{-10} Torr) equipped for low-energy electron diffraction (LEED), Auger electron spectroscopy (AES), ion sputtering and adsorption/desorption measurements utilizing both conventional and laser-induced heating methods. Details of the apparatus are published elsewhere [38]. The Pd(111) crystal is cleaned by repeated cycles of Ar^+ bombardment and by heating in the presence of oxygen. Thiophene, furan and pyrrole are purchased from Aldrich Chemical Company (99+%). Each are further purified by several freeze–pump–thaw cycles and determined free of impurities by gas-phase, mass spectral analysis. The Pd sample is cooled to 100 K and then dosed with the various reagent gases by backfilling the chamber.

Exposures (L = Langmuir = 10^{-6} Torr s) have been corrected for ion gauge sensitivities. The sensitivity factor for furan (3.29) is estimated using the value listed for tetrahydrofuran [39]. Thiophene (4.8) was estimated by calculating the ratio of values for 2-methylpropanethiol and *i*-butyl alcohol, then multiplying this factor by the value for tetrahydrofuran [39]. An analogous method was used to estimate the value for pyrrole (3.5), substituting the value for 2-

methylpropanethiol in the above calculation with that of isobutyronitrile from the same reference. The values used for reaction products were either obtained directly from reference or assumed to be unity based on the values listed for similar molecules: 1,3-butadiene (2.9) [40], CO and HCN (1.0) [39].

One of our most useful experiments is the *LITD survey*. During these experiments, the entire Pd sample is resistively heated to a selected temperature and allowed to equilibrate for 1 min before firing the laser. Each spectrum is obtained from a single laser shot, aimed at a different spatial position on the surface (laser spot size $\approx$ 1 mm^2). As the figures in the following sections will illustrate, each spectrum obtained is a complete mass spectrum of all the ions present in the cell. Several spectra are taken at each temperature and the signal magnitudes averaged. The LITD/FTMS signals are typically proportional to the surface concentrations for each species [38], therefore, relative yield information can be obtained from a single spectrum. Like conventional TPR, data from these surveys are displayed as a profile plot and describe the evolution of molecular species on the surface as a function of temperature. In contrast, however, the emphasis with LITD is not on what is coming *off* the surface, but rather, what is still *on* the surface. For this reason, these two techniques compliment one another and their usefulness in this manner is exploited in the following discussions.

In a typical FT-TPR experiment, the sample is resistively heated at a rate of approximately 3–5 K s^{-1}. In contrast to the LITD survey, the temperature of the sample is not allowed to equilibrate at any point during the experiment. Instead, the temperature is ramped beyond the point where the reaction is considered complete. Neutrals are driven into the gas phase upon reaching their thermal desorption temperature. The mass spectrometer then samples the ions present in the cell at a rate of 2 Hz. The data is displayed in much the same manner as in a LITD survey. Although each data point does not represent an average of signal magnitudes obtained at each temperature, the mass spectrometer is sampled at such a high rate that ΔT is kept small and many more measurements can be made at different temperatures.

RESULTS

Thiophene

Fourier transform mass spectrometry temperature programmed reaction (FT-TPR) studies at heating rates of approximately 3 K s^{-1} show only the desorption of a small amount of thiophene (exposure = 0.2 L corrected, desorption temperature = 220 K); no evidence of 1,3-butadiene desorption is observed. H_2 is a likely reaction product in the decomposition of thiophene, however, the fate of this species in either the LITD or TPR experiments is uncertain at this point. H_2^+ cyclotrons at a frequency outside the bandwidth of our analog-to-digital converter when using a magnetic field appropriate for detection of products such as thiophene and 1,3-butadiene (0.5 Tesla). As a result, separate experiments must be performed with a lower magnetic field strength ($\sim$0.1 Tesla) in order to observe m/z 2. These experiments are under way.

Figure 1 shows the signal intensities from the LITD/FT mass spectra for thiophene (m/z 84) and 1,3-butadiene (m/z 54) as a function of sample temperature after a 0.2 L exposure of thiophene. This exposure corresponds to a few percent of a monolayer, as determined by AES and flux calculations. Shown in Figs 2(a) and (b) are two individual LITD/FT mass spectra from the set in Fig. 1, at 230 and 320 K, respectively. These data clearly illustrate the loss of thiophene followed by the formation of 1,3-butadiene at 280 K. (These are not stick plots, but are true representations of the resolution and signal-to-noise obtained using this technique.) It is important to note that 1,3-butadiene is the only reaction product observed using LITD. Spectra taken at 100–200 K (not shown) are identical to Fig. 2(a), obtained after warming the sample to 230 K. These spectra are essentially the same as the gas-phase spectra obtained while dosing with thiophene. Above 230 K the thiophene signal decreases, disappearing completely by 350 K. Figure 2(b) was obtained after heating the sample to 320 K. In addition to a small amount of residual thiophene, peaks appearing in this spectrum are indicative of 1,3-butadiene; the fragmentation pattern in this spectrum matches published EI mass spectra for gas-phase 1,3-butadiene [41], as well as LITD/FTMS spectra for 1,3-butadiene on Pd(111) at low temperature obtained in this laboratory [42]. Above 380 K, the 1,3-butadiene signal vanishes due to decomposition (Fig. 1). [We have observed that,

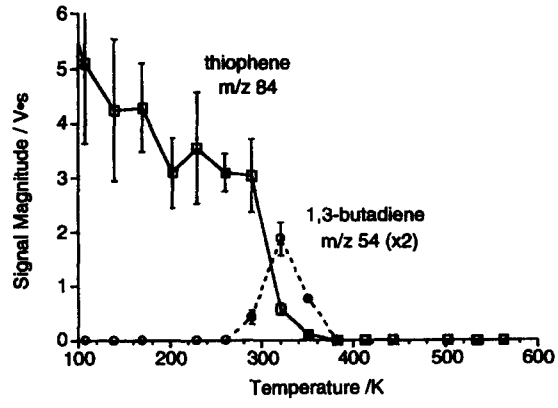

Fig. 1. An LITD survey of a 0.2 L exposure of thiophene on Pd(111) dosed at 100 K. The plot shows a decay in thiophene (m/z 84) accompanied by the growth of 1,3-butadiene (m/z 54). The 1,3-butadiene signal has been increased by a factor of 2. Quantitative comparison in terms of thiophene and butadiene relative concentrations requires correction for electron beam sensitivities and fragmentation. See the text.

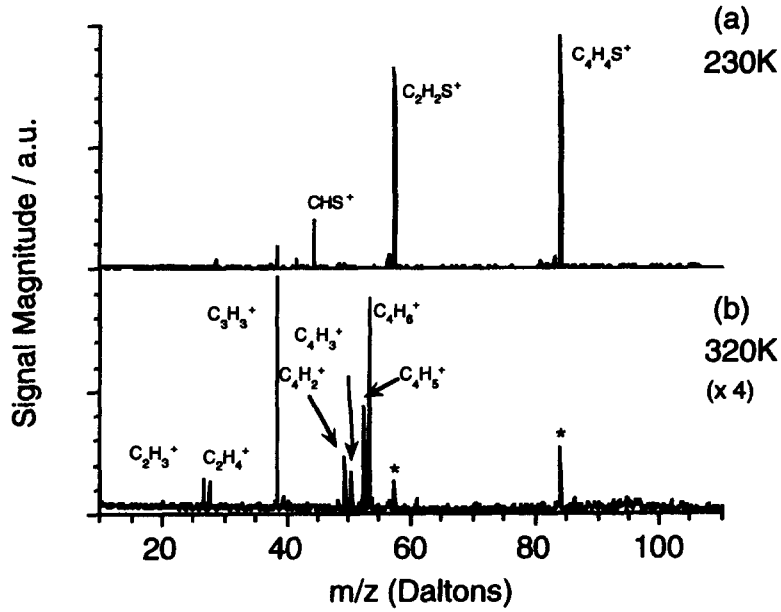

Fig. 2. Selected individual LITD/FT mass spectra from those profiled in Fig. 1. (a) After warming the sample to 230 K, the spectrum indicates a significant amount of thiophene remaining on the surface (primarily m/z 39, 45, 58 and 84). (b) Heating to 320 K produces 1,3-butadiene. The signal has been increased by a factor of 4. The asterisks in spectrum (b) denote m/z peaks 58 and 84, which are due to residual thiophene on the surface.

on clean Pd(111), 1,3-butadiene (0.3 L) is stable for several minutes at temperatures as high as 325 K, but decomposes above 350 K [42].]

Our results on Pd(111) show that, at low temperatures, thiophene adsorbs molecularly. Heating the surface to *ca* 300 K results in the complete loss of thiophene and formation of a small amount of 1,3-butadiene, which must involve hydrogenation. (Some small amount of surface hydrogen is always present from the background and more may be provided by decomposition of adsorbed hydrocarbons, therefore, no deliberate coadsorption of hydrogen was necessary or employed.) Two competing mechanisms have been proposed for hydrodesulfurization of thiophenes [13,43]. They differ primarily in the relative timing of hydrogenation and sulfur abstraction. The two proposed mechanisms are illustrated in Scheme I. In the top mechanism, hydrogenation of thiophene precedes C—S bond scission, while in the bottom mechanism C—S bond scission occurs first. If the reaction proceeds *via* the top pathway, we would expect to see virtually all of the thiophene that reacts before 320 K end up as adsorbed 1,3-butadiene, since our previous results show that 1,3-butadiene is stable on Pd(111) at 320 K. In contrast, if the bottom mechanism predominates, then the yield of 1,3-butadiene could be much lower. In this mechanism, hydrogenation of C_4H_4 to 1,3-butadiene competes with further dehydrogenation of the C_4H_4 intermediate. With this mechanism in mind, it is also possible that addition of a single hydrogen activates C—S bond cleavage leaving C_4H_5 on the surface which can then dehydrogenate to give hydrogen and adsorbed carbon at higher temperatures. This, in turn, could also lead to relatively low yields of 1,3-butadiene, depending on the branching between hydrogenation and dehydrogenation.

As mentioned in the preceding (experimental) section, the data points that appear in the LITD surveys represent an average of the signal magnitudes of several spectra taken at each temperature. The LITD/FTMS signals are typically proportional to the surface concentrations for each species, therefore, relative yield information can be obtained from even a single spectrum. However, large ion densities, approaching the limits of the ion trap, can lead to instabilities in the signal magnitudes. Such fluctuations are reflected in the large error bars associated with the low-temperature data points of Fig. 1. It would appear that the signal for thiophene decreases steadily from its adsorption temperature (100 K) up to the point at which it decomposes (300 K), although the onset of thermal desorption (from prior TPD studies) does not occur until 200 K. However, the downward trend is within the error bars in that region of the survey. Within these uncertainties, any downward trend in signal intensity before the desorption onset for thiophene may be indicative of decomposition to the C_4H_4 intermediate, but at a temperature where hydrogenation to 1,3-butadiene is not yet efficient and, therefore, not observed.

Based on the preceding argument, it is necessary to have some quantitative measure of the amount of thiophene which decomposes relative to the amount that desorbs. If a significant portion of thiophene decomposes, then the relative amounts of 1,3-butadiene-formed *vs* thiophene-consumed should give

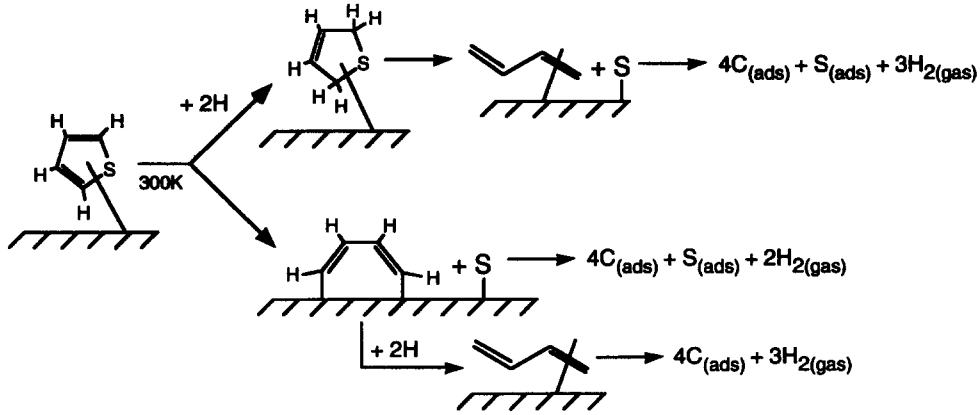

Scheme I.

some indication of the dominant mechanism. One can estimate the relative amounts of reversibly and irreversibly adsorbed thiophene using a combination of FT-TPR and LITD/FTMS experiments. This experiment was identical to those previously described above, except for two differences: (1) a small amount (a few percent of a monolayer, as determined by AES and flux calculations) of S was present and (2) a small amount (estimated 3% of a monolayer from thermal desorption curves) of CO was present. The amounts of thiophene and 1,3-butadiene observed by FT-TPR and LITD/FTMS were unchanged, so the chemistry is presumably identical. In these experiments, the small amount of CO coadsorbed can be used as an internal calibrant to determine the relative amounts of thiophene reversibly and irreversibly adsorbed. This is because all of the adsorbed CO eventually desorbs during slow heating in the TPR from clean Pd(111) [44] and we assume that all of the CO desorbs during laser heating, as evidenced by the lack of signal from subsequent laser shots at the same spot. Thus, the CO signal from an LITD/FTMS experiment and the integrated area for a CO FT-TPR experiment should both represent the total amount of adsorbed CO and therefore be equivalent. The ratio of these two signals, then, gives a scaling factor to relate the LITD signal magnitude to the TPR integrated signal. We can use this scaling factor to compare the LITD and TPR signals for thiophene to obtain a lower limit for the amount of thiophene that decomposes during slow heating. We again assume the LITD from a cold surface gives us a measure of the total amount of thiophene initially adsorbed and then TPR measures the amount that desorbs intact. Using this approach, we estimate that 85% of the adsorbed thiophene reacts on the surface and only 15% desorbs. This treatment assumes that CO and thiophene have similar desorption efficiencies using LITD. In fact, thiophene is more likely to undergo some decomposition, if any, during LITD. Also, the *bulk* sample temperature histories are quite different for the TPR and LITD experiments, so the competition between desorption and decomposition of the thiophene might be different for the two experiments. In fact, the average *bulk* sample heating rate is much faster for TPR (3 K s^{-1}) compared with an LITD survey (<1 K s^{-1}). Thus, one might expect that TPR would yield a larger fraction of thiophene desorption than during the course of an LITD survey study. Both of these limitations would imply that the ratio of irreversibly adsorbed to reversibly adsorbed thiophene, estimated using these values, is a lower limit and perhaps significantly more than 85% decomposes. Of course, the branching ratio between desorption and decomposition could change with the initial coverage of thiophene. The study presented here was conducted at submonolayer coverages. In such a concentration regime there is very little competition for adsorption sites, which otherwise could be a limiting factor for decomposition. At higher coverages, these sites would be occupied by adsorbates, possibly hindering reactions requiring additional adsorption sites or requiring surface mobility. Our coverage dependent studies of thiophene on clean Pd have yet to render any significant changes at submonolayer coverages, although investigations are ongoing.

We can estimate the relative yield of 1,3-butadiene from thiophene on clean Pd(111) using the LITD signals for the maximum surface concentrations for the two species. Peak magnitudes of the most intense signals for thiophene ($T = 110$ K) and 1,3-butadiene (at $T = 320$ K) from the LITD data in Fig. 1 are used. Both thiophene and 1,3-butadiene yields are corrected for ion gauge sensitivities as an estimate of the relative sensitivity by electron ionization in the mass spectrometer [45]. By 320 K, approximately 90% of the thiophene signal has been lost and, from our CO coadsorption data described above, we can state that, at most, 15% of the initial thiophene is lost to desorption. Thus, as least 75% of the initial thiophene adsorbed has decomposed on the surface by 320 K. The corrected 1,3-butadiene yield at 320 K is approximately 30% of the initial thiophene signal. Since this is substantially less than 75%, our data implies that the bottom mechanism in Scheme I is the most likely

of the two. (However, addition of a single hydrogen followed by C—S bond scission to leave C_4H_5 is also possible.) In addition, however, a signal for 2,5-dihydrothiophene might be expected if the top mechanism were important. In neither FT-TDS nor LITD/FTMS was any such signal observed. Thus, the top mechanism is inconsistent with our data. Our data imply that S-abstraction precedes formation of 1,3-butadiene on Pd(111).

If C—S bond scission occurs first, then the formation of S and a C_4H_x ($x = 4$ or 5) intermediate on the surface is implied. A C_4H_4 species has been proposed by several groups as the intermediate species in acetylene cyclotrimerization on Pd(111) [46–52]. Likewise, several studies involving thiophene decomposition on Ni, Re and Mo surfaces suggest an intermediate C_4-metallocycle species as well [13–17]. Hydrogenation of the C_4H_x intermediate leads to the formation of 1,3-butadiene. 1,3-Butadiene is also a product in most HDS studies of thiophene, however, only in the presence of excess hydrogen ($P_{H2} \geqslant 780$ Torr) [18,53,54]. Using TPR, small quantities of 1,3-butadiene from thiophene decomposition have previously been observed on clean Ni(111) [55] and Pt(100)5 × 20 [56], however, only at saturation coverages of thiophene. At low coverages of thiophene (0.2 L) we see no 1,3-butadiene from Pd in our TPR spectra, similar to what has been observed for low coverages of thiophene on Ni(111) [55] and Pt(100)5 × 20 [56]. However, using LITD we do observe 1,3-butadiene following low exposures of thiophene on Pd(111). This clearly demonstrates one of the limitations of TPR where adsorbates formed in the initial stages of a reaction are not observed if they decompose before desorbing from the surface. In this situation a technique such as LITD is necessary in order to observe these intermediates and to further elucidate the mechanism of such reactions [29–32]. (It is not possible, using this data, to rule out the possibility that the formation of 1,3-butadiene only occurs as a result of laser heating. Were this the case, it would be even stronger evidence for the conclusions regarding the preferred mechanism presented above. However, it is unlikely that the addition of two hydrogen atoms at a C_4H_4 intermediate would be so efficient during laser heating [53].)

The surface reactivity of thiophene varies significantly depending on the type of metal used. In contrast to these Pd results, other late transition metals, such as clean Cu(100) [19] and Ag(111) [54] have been shown to adsorb thiophene reversibly with no other desorption products observed during TPR. The reversible pathway competes with the decomposition of thiophene on clean Mo(100) [57,58] and (110) [59] surfaces, as well as on Ni(111) [47], Re(001) [60] and Si(111)2 × 1 [61]. It has also been shown that Ni- and Co-promotion of Mo and W surfaces increases HDS activity [62–65]. Given this, it is reasonable to suggest that other group VII and VIII metals, such as Pd, would also serve as effective promoters on HDS catalysts. Furthermore, transition metal sulfides of Pd have been shown to catalyze HDS more than an order of magnitude more efficiently than sulfides of Co and Ni [66]. HDS activity for sulfided synergic pairs, like Ni/W and Co/Mo, have been shown to dramatically improve HDS acitivty over their respective "unpromoted" individual sulfides. It seems reasonable to suggest then, based on the comparison of activities mentioned above, that Pd/W or Pd/Mo would have improved activities as well, perhaps surpassing the quality of the synergic contacts used most often today (i.e. Ni and Co promoted sulfides of W and Mo). To the best of our knowledge, though, investigations of Pd promotion of W or Mo sulfides have not yet been published.

Furan

TPR studies are performed using a 0.3 L exposure of furan and a heating rate of 3K s^{-1}. Again, these studies use FTMS, hence, a complete mass spectrum (m/z 10–650) of desorbing species is obtained every 2 s. The only species observed are furan, H_2 and CO ($T_{max} = 265$, 360 and 450 K, respectively). To estimate the relative yield of reversibly *vs* irreversibly adsorbed furan, the integrated areas under the thermal desorption traces are calculated for CO (m/z 28) and furan (sum of m/z 39 and 68 areas). The furan total is corrected using the ion gauge sensitivity as an estimate of the relative sensitivity by electron ionization in the mass spectrometer. The ratio of the m/z 28 area relative to the corrected total of m/z 29, 39 and 68 is approximately 0.4, indicating that 40% of the initial coverage of furan decomposes to yield CO. Direct formation of CO from furan has been observed on Mo(100) and Mo(110) surfaces, also [67].

Figure 3 shows the signal intensities from the LITD/FT mass spectra for furan (m/z 68), CO (m/z

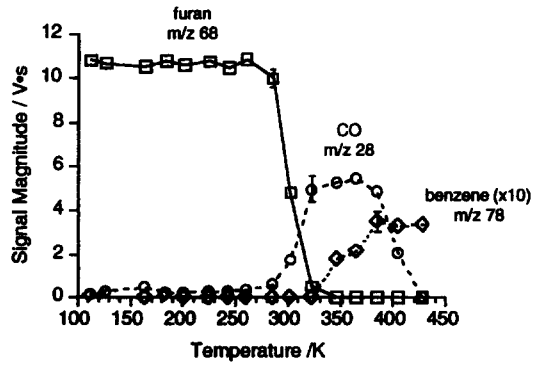

Fig. 3. An LITD survey of a 0.3 L exposure of furan on Pd(111) dosed at 100 K. The plot shows a decay in furan (m/z 68) followed by growth of CO (m/z 28) and then benzene (m/z 78). The benzene signal has been increased by a factor of 10. Several spectra are obtained at each temperature and error bars are displayed for the one data point with the largest scatter within each set.

28) and benzene (*m/z* 78) as a function of sample temperature after a 0.3 L exposure of furan. Shown in parts (a) and (b) of Fig. 4 are two individual LITD/FT mass spectra from the set in Fig. 3, at 260 and 385 K, respectively. These data clearly illustrate the loss of furan accompanied by the growth of CO at 280–320 K followed by the formation of benzene above 350 K. Spectra taken at 100–240 K (not shown) are identical to Fig. 4(a), obtained after warming of the sample to 260 K. These spectra are essentially the same as the gas-phase spectra obtained while dosing with furan. In addition, however, a small peak at *m/z* 28 is observed and maintains a constant magnitude from 100 to 260 K. This may be CO deposited during furan adsorption (displaced from the chamber walls) or be due to low-temperature furan decomposition at defect sites. Above 280 K, however, the furan signal decreases as the CO signal increases, plateauing by about 320 K. Figure 4(b) was obtained after heating of the sample to 385 K. The peak appearing at *m/z* 78 indicative of benzene and first appears at 350 K. [No benzene is observed in TPR. Since previous studies show that benzene exposures of less than 0.25 L (where ~3 L leads to saturation) would decompose on Pd(111) before desorbing [68] and our LITD signals for benzene are indicative of coverages less than one would achieve with a 0.25 L exposure, the benzene produced is only observed because the laser heating favors direct desorption.] Above 380 K, the CO signal decreases due to depletion by conventional desorption.

By 320 K, the furan signal has almost completely disappeared and CO formation is essentially complete. Presumably, by 320 K, C_3H_3 formation is also essentially complete; however, we see no evidence for this species in LITD. (All of the *m/z* 39 observed can be attributed to furan and no *m/z* 39 is observed unless *m/z* 68, the parent furan mass, is also observed.) It is important to note that benzene formation occurs at a temperature much higher than the temperature at which furan was lost, which supports the presence of a stable intermediate on the surface. This species, most likely C_3H_3, is probably too tightly bound or too labile to be desorbed intact, even with rapid laser heating. These experiments were carried out three times with identical results, as illustrated in Scheme II.

FTMS monitors all masses from *m/z* 10 to 650 simultaneously, and all observed mass peaks in our study of furan on Pd(111) can be attributed to furan, CO, hydrogen and benzene. No C_4 species are observed. However, the stability of a C_3H_3 species on the surface is rather unexpected. Studies of furan HDO over supported Mo/C catalysts show C_4 species as the major products [12]. HDS of thiophene on Mo or W catalysts results in only C_4 species [18] and our results for thiophene decomposition on Pd(111) show exclusively C_4 products using LITD/FTMS and FT-TPR [69]. The formation of furan from adsorbed oxy-

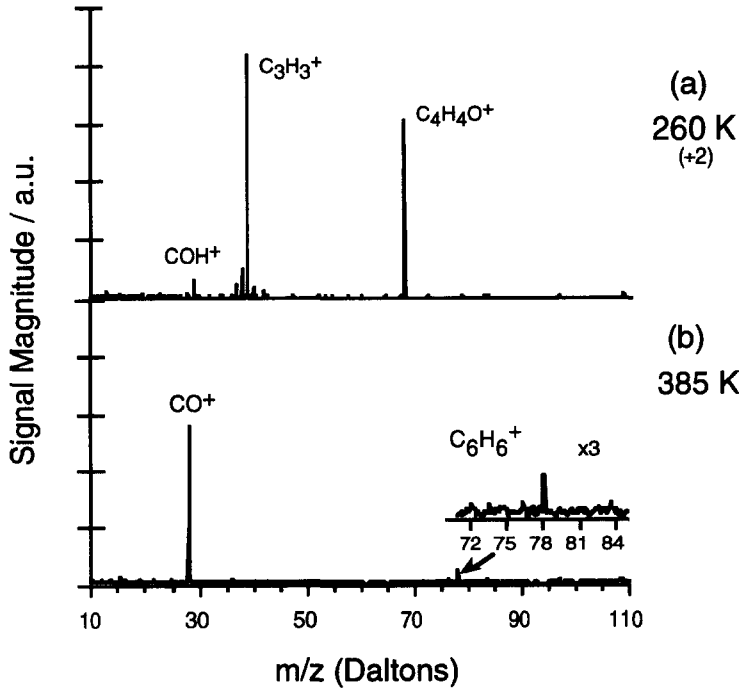

Fig. 4. Selected individual LITD/FT mass spectra from those profiled in Fig. 3. (a) After warming the sample to 260 K, the peaks indicate a significant amount of furan remaining on the surface (primarily *m/z* 29, 37, 38, 39 and 68) with a trace amount of CO (*m/z* 28). The entire spectrum has been scaled down by a factor of two in the intensities. (b) Heating to 385 K produces a peak at *m/z* 78 (benzene) and increased CO. The insert shows the region around *m/z* 78 with signals enhanced by a factor of 3.

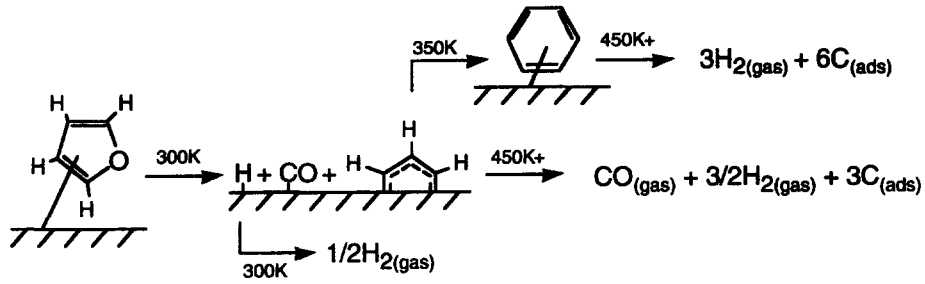

Scheme II.

gen and acetylene on Pd(111) is also believed to occur *via* a C_4H_4 intermediate [70]. The exclusive production of CO, H and the C_3H_3-derived benzene from furan is, therefore, an unexpected result. However, Gellman *et al.* [18] and Furimsky [7] both report that furan HDO on Mo-based catalysts does produce some C_3 product (primarily propene); however, Furimsky's data show that C_4 species are dominant by a factor of 3–5 over C_3 products. A recent study by Ormerod *et al.* has confirmed many of these findings [71].

In an attempt to confirm the presence of this C_3H_3 species as a precursor to benzene formation, furan decomposition was monitored using a mixture of proteated and deuterated furans. A solution containing both C_4D_4O and C_4H_4O was premixed in a 60:40 ratio prior to being placed on the vacuum line (this ratio was confirmed by gas-phase mass spectral analysis). This eliminated the need for any pre- *vs* post-dosing procedures. (The odd ratio is an artifact of sample preparation and not the result of a deliberate attempt.) Figure 5 is the profile plot, similar to the one shown in Fig. 3, of a C_4H_4O/C_4D_4O mixture adsorbed to Pd(111) using a slightly higher exposure than is shown in the previous figure. Scheme III is a proposed mechanism consistent with our observations. If benzene formation proceeds *via* coupling of the two C_3H_3 fragments, one would expect to observe signals for benzene containing D and H in multiples of three (i.e. C_6D_6, $C_6D_6H_3$, C_6H_6 in a 2:3:1 ratio). Indeed, a significant signal for *m/z* 81 ($C_6D_6H_3$) appears first in this spectrum, however, no signals for C_6H_6 or C_6D_6 are observed (presumably because their signals were in the noise). Not surprisingly though, other mass peaks (*m/z* 80 and 82) are observed at higher temperatures, which can be attributed to H/D exchange occurring on the surface. This is quite common on late transition metal surfaces [72]. To prove these species were formed as a result of H/D exchange, only the perdeutero furan was adsorbed onto the surface (with adventitious hydrogen) as an exposure comparable to that used in the perproteo study. In this experiment we observed primarily C_6D_6 (*m/z* 84), but also see evidence for exchange of one (C_6D_5H, *m/z* 83) and even two hydrogens ($C_6D_4H_2$, *m/z* 82). These

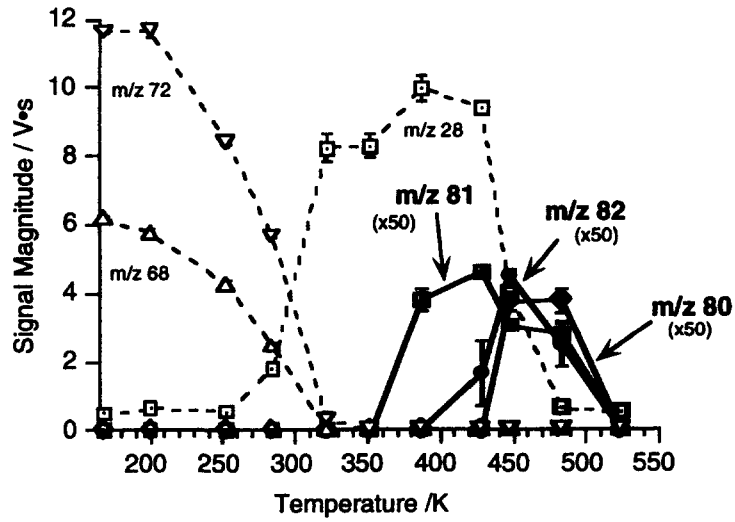

Fig. 5. An LITD survey of a mixture of proteated and deuterated furan (60:40 of $C_4H_4O:C_4D_4O$) using a 0.76 L exposure at 100 K. A significant signal for $C_6D_3H_3$ (*m/z* 81) appears first in the spectra. Peaks for $C_6D_4H_2$ (*m/z* 82) and $C_6D_2H_4$ (*m/z* 80) appear at slightly higher temperatures which is attributed to H—D exchange occurring on the surface. Signal magnitudes for these three species have been increased by a factor of 50.

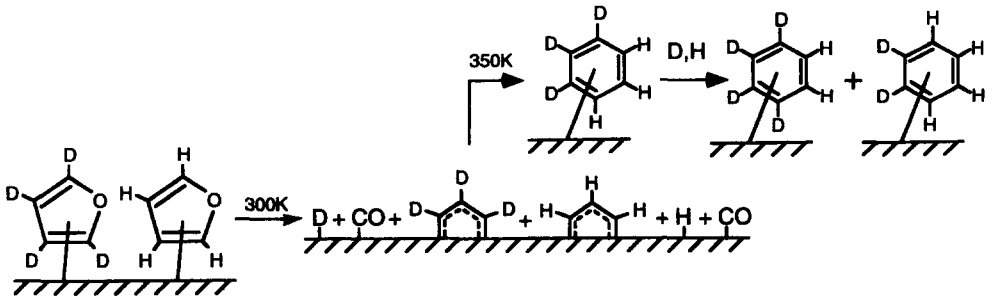

Scheme III.

results are all consistent with a mechanism for benzene formation which proceeds *via* coupling to two C_3H_3 fragments.

One might question whether laser heating drives some intermediate (such as a metallacycle with a C_6H_6 component) to benzene before or during desorption. Due to its rapidity, however, laser heating is likely to produce only subtle changes in the desorbing species [53]. Thus, changes in the LITD mass spectra as surface temperature is varied can still be correlated with changes in surface composition. Laser-driven recombination of C_3H_3 can be ruled out, since, if laser-driven recombination of two C_3H_3 species were an efficient process, benzene desorption would have been observed at 320 K when most of the C_3H_3 had formed. Clearly, something about the surface composition changes between 320 and 350 K. Our data indicate that C_3H_3 is stable for many minutes between 320 and 350 K on Pd(111). At 350 K, these species are able to dimerize to form a species similar, if not identical, to adsorbed benzene. The barrier to this process may be due to diffusion of the C_3H_3 or to bond breaking between the fragments and the Pd surface. Our current data cannot distinguish between the two. As mentioned before, it is somewhat surprising that C_3H_3 would be stable and mobile at these temperatures on group VIII metals, considering their dehydrogenating nature. Typically, alkyl fragments are only observed to recombine on coinage metals [73] (although methyl coupling to yield C_2 species has been observed on other late transition metal surfaces, including Pd, following the photodissociation of methyl halides [74–76]). Also, examples of stable C_3 species incorporated into organometallic clusters have been identified as products from alkyne–alkylidyne coupling as well as reactions of alkenes, alkynes and dienes with metal clusters [77–79].

The data from LITD (see Fig. 3) can be used to determine the relative yields of furan, CO and benzene by making assumptions about the relative efficiency of laser-induced desorption for each species. Assuming that the efficiency is the same for each, we calculate that 60% of a 0.3 L exposure of furan decomposes to give CO (plus H and, presumably, C_3H_3) and 2% of the furan ends up as benzene. Thus, approximately 3% of the C_3H_3 species (assuming that CO and C_3H_3 are formed in equal quantities) form benzene; the remainder decompose on the surface. A coverage-dependent study revealed that these relative amounts did not vary significantly through a range of exposures (0.3–1.0 L, corrected). However, the benzene yields reported here are lower limits, since furan and CO are likely to have higher efficiencies for laser-induced thermal desorption than benzene. Both CO and furan desorb at lower temperatures (430 and 280 K, respectively, in TPR) than does benzene (520 K). In fact, as mentioned above, low coverages of benzene decompose completely in TPR. Therefore, the efficiency of thermal desorption in LITD is likely to be smallest for benzene [30]. Furthermore, the possibility of defect sites inducing the formation of benzene in such low yields may be argued; however, it is difficult to conceive how a defect would lead to benzene formation, since defects are usually associated with higher binding energies and enhanced decomposition.

Separate experiments were performed with a lower magnetic field strength ($\sim$0.1 T) to observe m/z 2 (see discussion regarding H-detection in experimental section). These experiments follow the same procedures outlined above; however, a slightly higher exposure (0.5 L) of furan is used (saturation requires $\sim$2 L [80]). TPR (3 K/s) shows H_2 evolution beginning at $\sim$300 K with the desorption peak centered around 360 K with a broad tail to significantly higher temperatures. (Hydrogen on clean Pd(111) desorbs with a peak centered at 310 K using a heating rate of 25 K s^{-1} [46].) Using LITD, no significant signal for H_2 is observed after heating a furan-dosed Pd(111) surface. (Experiments on the dehydrogenation of cyclohexene on Pd(111), performed on the same day, did show a strong signal for H_2 from surface H using the same conditions described here.) The results from TPR and LITD indicate that H_2 evolution in TPR of furan on Pd(111) is rate limited by CH bond breaking. Ormerod *et al.* also observed a desorption maximum for H_2 at 350 K with a broad tail, but identified smaller features at 420 and 520 K after low-temperature adsorption of furan on Pd(111) [71].

In contrast to these Pd results, other late transition metals, such as clean Cu(110) [19] and Ag(110) [20], have been shown to adsorb furan reversibly with no

other desportion products observed during TPR. It has also been shown that Ni and Co are more effective than Zn in the promotion of Mo and W HDO catalysts [81]. It appears, then, that the Co and Ni group metals should be expected to be more effective promoters than the Cu and Zn group metals. However, furan coadsorbed with oxygen on Ag(110) has been shown to produce CO_2 and H_2O, both of which are evolved starting at about 300 K during TPR [21]. At higher temperatures (520 K), very small amounts of partial oxidation products, such as maleic acid, benzene and bifuran, are evolved [21]. In these studies, benzene formation was also attributed to the cycloaddition of two C_3H_3 fragments, but only after oxidative activation of furan decomposition. The Pd surface used in our study does not require this highly oxidative environment. Furthermore, whereas HDO of furanic species over typical hydrotreating catalysts requires temperatures in excess of 670 K, Pd catalyzes rapid deoxygenation at 300 K. This may point to the fundamental action of late transition metal promoters in HDO catalysts. Our results also show, however, that significant amounts of carbonaceous material may be left behind on the Pd surface. These species may act to poison further catalytic reactivity unless removed, e.g. by hydrogen supplied to the feed.

Pyrrole

The low-temperature reaction of pyrrole on clean Pd(111) is shown in the LITD survey in Fig. 6. This figure shows that a 0.3 L exposure of pyrrole, adsorbed at low-temperature, is relatively stable on the surface from 100–230 K. Above 230 K, the intensity drops by more than a factor of 10, disappearing from the spectra completely by 370 K. The continuous loss of signal for pyrrole in LITD would suggest a competition between desorption and decomposition, however, the FT-TPR spectra in Fig. 7 indicates very little desorption of pyrrole. Pyrrole appears, then, to be reacting at these low temperatures and is less stable than either of its two analog species, thiophene or furan. After heating the surface to 270 K, a signal for HCN (m/z 27) is observed in LITD (Fig. 6) and persists until 500 K (this point is not shown in Fig. 6, but has been confirmed by subsequent LITD experiments). The loss in signal at 500 K is due to thermal desorption, as shown in Fig. 7. The desorption peak for HCN in Fig. 7 is quite substantial in comparison to the signal for pyrrole. It appears that most, if not all, of the pyrrole present at 100 K reacts on the surface to form HCN. By using the TDS and LITD data, correcting for ionization efficiency and fragmentation, greater than 90% of the pyrrole decomposes to give HCN. The desorption trace of HCN in Fig. 7 is relatively broad with two distinguishable peaks, though overlapping, centered at 540 and 650 K. This is much higher than the thermal desorption temperature of HCN adsorbed on clean Pd(111), which occurs in a single, narrow peak at 425 K (HCN adsorbed at or below temperatures of 120 K desorbs at this temperature as well, in addition to forming multilayers which begin desorbing at 140 K) [82]. This shift to higher temperatures suggests that the presence of HCN in the gas phase is reaction limited and not desorption limited. However, in LITD, a signal for m/z 27 is observed at temperatures above and below its thermal desorption temperature! Based on these results, it appears that HCN is reactively formed, perhaps by thermal (or laser-induced thermal) decomposition of some intermediate species. Separate experiments were performed at a lower magnetic field strength ($\sim$0.1 Tesla) in order to detect the evolution of hydrogen from this reaction. The LITD results are shown in Fig. 8. This survey indicates that H_2 is present on the surface from 200–300 K. Above 300 K,

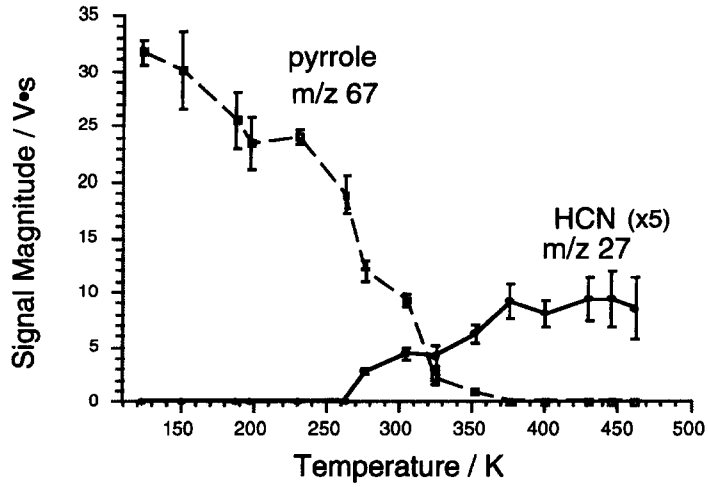

Fig. 6. An LITD survey of a 0.3 L exposure of pyrrole on Pd(111) dosed at 100 K. The plot shows a decay in pyrrole (dashed line) followed by the growth of a signal for HCN (solid line). Values have been corrected for electron beam sensitivities and fragmentation (see text).

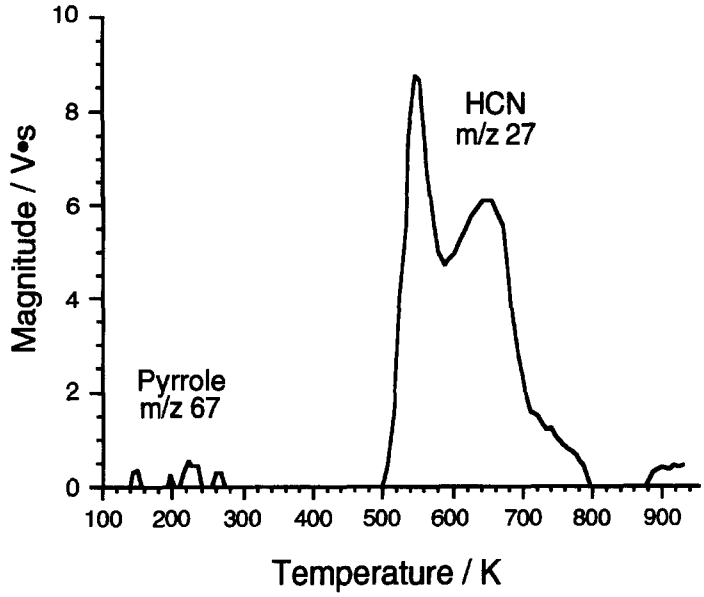

Fig. 7. An FT-TPR spectra of a 0.3 L exposure of pyrrole on Pd(111) using a heating rate of 3 K s^{-1}. Very little pyrrole desorbs (dashed line). The large signal for HCN (solid line) indicates virtually all of the pyrrole decomposes to liberate HCN.

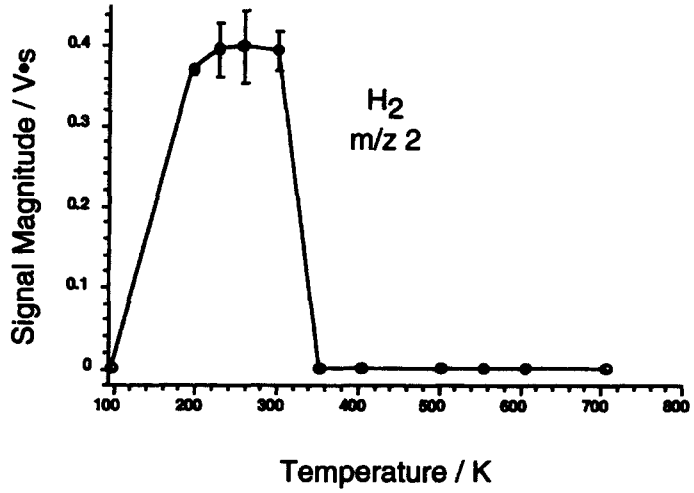

Fig. 8. An LITD survey of H_2 evolved from a 0.3 L exposure of pyrrole on Pd(111). (The magnetic field is reduced to ~0.1 T in order to observe this signal.) H_2 is present on the surface from 200 to 300 K, after which it thermally desorbs from the surface.

any hydrogen present on the surface of Pd(111) will thermally desorb [83]. The first maximum in the TPR spectrum for H_2 desorption from pyrrole decomposition (Fig. 9) is consistent with this observation. The desorption trace in Fig. 9 contains three peaks centered at 315, 450 and 510 K. The peak structure, particularly the magnitudes, are significantly different than that observed for furan [71]. H_2 desorption from the decomposition of hydrocarbons on Pd(111) begins at 450 K and extends to 830 K [46], so presumable the higher temperature peaks in Fig. 9 are due to pyrrole fragments which have further decomposed. However, we believe the low-temperature peak is due to the desorption of the hydrogen bonded to the nitrogen of pyrrole.

A small signal for m/z 28 (not shown) is the only other species observed in this study, which is due, we believe, to background CO and CO displaced from the chamber walls. LITD and TPR results combined indicate that this m/z 28 species is present on the surface at temperatures below 300 K, with desorption centered at 480 K [which is consistent with what we have observed for CO on clean Pd(111)]. Unless reactively formed, it is unlikely that either N_2 or C_2H_4 (both m/z 28) would be responsible for the signal observed, since both thermally desorb from Pd(111)

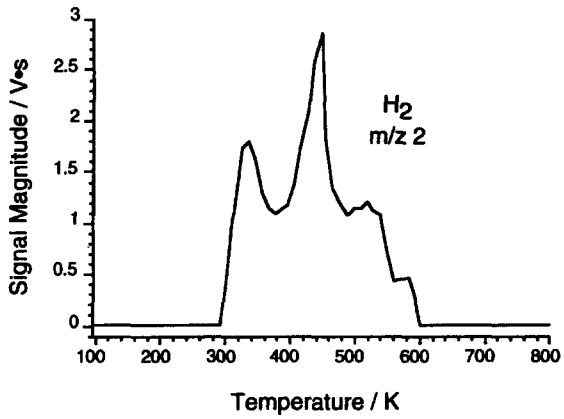

Fig. 9. An FT-TPR spectra of H_2 evolved from a 0.3 L exposure of pyrrole on Pd(111) at 100 K. The desorption trace contains three peaks (plus a shoulder at high temperature) centered at 315, 450 and 510 K. The low-temperature peak is desorption-rate limited and is most likely due to the desorption of the hydrogen bonded to the nitrogen of pyrrole, while the higher temperature peaks are due to pyrrole fragments which have further decomposed.

before 300 K [84,85]. To further rule out the possibility of a hydrocarbon species, such as C_2H_4 or even CNH_2 (both m/z 28), the LITD experiment was repeated using pyrrole-d_5 (Aldrich 98%). No shift was observed for m/z 28; if either of these two species were present, one would expect a signal at m/z 32 or 30, respectively, and neither were observed.

These results, although preliminary, have proposed as many questions as they have yielded answers. These results suggest, however, that pyrrole decomposition does not proceed through a C_4H_4 intermediate, as in the case of thiophene. Given the stability of C_4H_4, it is unlikely that it would undergo C—C bond cleavage at such low temperature to provide carbon atoms on the surface to form $CN_{(ads)}$ or $HCN_{(ads)}$. Furthermore, assuming there is ample hydrogen present on the surface following pyrrole decomposition, we would expect to see a signal for 1,3-butadiene if the reaction did proceed *via* C_4H_4 and none was observed. Moreover, the possibility of pyrrole reacting analogously to furan, losing 2H+CN and leaving C_3H_3 on the surface, seems just as improbable as the C_4H_4 intermediate pathway. If H and CN are present on the surface as low as 300 K, one can expect $HCN_{(ads)}$ to form at this temperature and subsequently desorb at 425 K [86]. A significant amount of pyrrole has decomposed before 300 K, which would provide enough $H_{(ads)}$ and $CN_{(ads)}$ to form $HCN_{(ads)}$. As discussed above, though, the presence of HCN is limited by some other reaction taking place above the thermal desorption temperature of HCN. In other words, there is no HCN present on the surface before 500 K and the signals for HCN observed in LITD at temperatures below 500 K are probably due to laser-induced thermal fragmentation of some surface intermediate containing HCN. In addition, no benzene formation was observed in the decomposition of pyrrole. This is in contrast to what is observed for furan decomposition.

The mechanism which we propose for pyrrole decomposition is shown in Scheme IV. Pyrrole appears to adsorb molecularly at low temperature (100 K), but readily decomposes as the surface temperature is increased. Results from the monitoring of H_2 suggest that the initial decomposition stage involves loss of the hydrogen atom located on nitrogen; H_2 is present on the surface during the temperature range that pyrrole is decomposing and neither furan nor thiophene lose hydrogen from C—H bond breaking below ~350 K. A LITD signal for H_2 was only observed in the case of pyrrole decomposition. Pyrrole is the only heterocycle of the three which contains an extra hydrogen (located on the nitrogen), thus, we believe the source of this signal to be the nitrogen hydrogen. At temperatures above 300 K, we believe the ring of pyrrole is opened forming some intermediate species containing HCN. HCN is readily cleaved from this intermediate species when subjected to laser-induced heating conditions, but remains mostly intact under slow-heating conditions until 500 K. Our results indicate the presence of some hydrocarbon species that decomposes above 325 K yielding hydrogen and above 500 K to give HCN. Scheme IV summarizes our proposed mechanism. At 500 K HCN is formed and subsequently desorbed, although our data suggests that the formation is not due to the recombination of $CN_{(ads)}$ and $H_{(ads)}$. No other significant desorption products are observed which suggests that the carbon backbone of the intermediate simply decomposes to $C_{(ads)}$ and $H_{(ads)}$ prior to or following the cleavage of HCN. This decomposition is also marked by the evolution of H_2 from 450 to 600 K. The nature of this intermediate may also explain the absence of benzene formation from recombination of C_3H_3.

CONCLUSIONS

Despite the similarities in their structures, thiophene, furan and pyrrole react very differently on a Pd(111) surface. With LITD, we show that the low-temperature decomposition of thiophene of Pd(111) proceeds *via* C—S bond scission forming a C_4H_x ($x = 4$ or 5) intermediate, which hydrogenates and desorbs as 1,3-butadiene. In TPR, however, we observe no signal for 1,3-butadiene. The cleavage between the C—S bonds of thiophene results in the deposition of sulfur which, due to the strong interaction between $S_{(a)}$ and Pd(111), remains on the surface even at elevated temperatures. Interestingly, a fundamental debate still exists over the mechanism of hydrodesulfurization with regards to the timing of the hydrogenation step relative to S-abstraction [87–89] and our results on Pd(111) support a pathway whereby, in the absence of excess hydrogen (other than

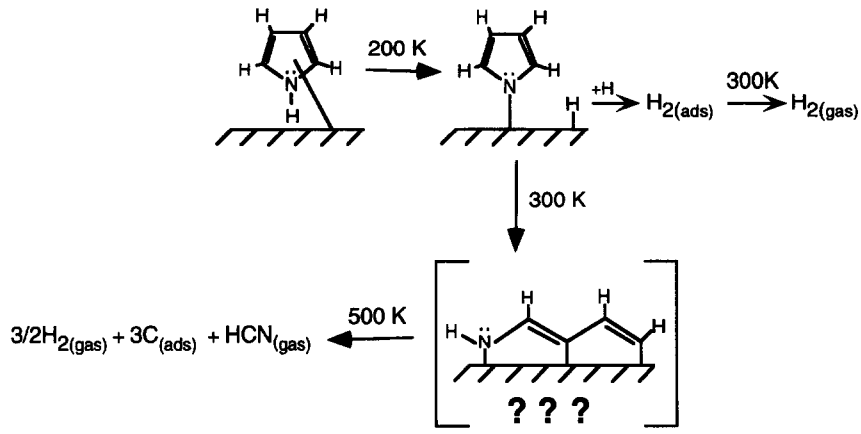

Scheme IV.

that which remains following the decomposition of thiophene), abstraction is followed by hydrogenation. However, in direct contrast to the case of thiophene, furan decomposition on Pd(111) is shown to proceed at low temperature *via* elimination of α-H and CO, leaving a C_3H_3 species on the surface. Heating to 350 K causes dimerization of the C_3 species, forming benzene [45]. This coupling of C_3 fragments was confirmed by the isotopic labeling studies involving a mixture of proteated and deuterated furans. The formation and subsequent desorption of CO from furan decomposition effectively and efficiently removes oxygen from the surface, which is contrary to what is observed for S in the decomposition of thiophene.

Preliminary results of pyrrole on Pd(111) indicate that decomposition occurs at a lower temperature than either thiophene or furan. In both LITD and TDS, HCN is the only product observed in this reaction. At first glance, the mechanism for decomposition appears analogous to that of furan decomposition; proceeding through a C_3 intermediate species. However, there is no evidence of benzene formation, even using LITD. This implies that no C_3H_3 species is formed before ~380 K, or we would expect some benzene formation in LITD spectra. Nor is it likely that adsorbed N and C_4H_X are formed, since we see no 1,3-butadiene. Nevertheless, on Pd(111) heteroatom removal in the decomposition of pyrrole is similar to that of furan, in that the formation and subsequent desorption of HCN removes a significant fraction of nitrogen from the surface.

With thermodynamic factors considered, one might expect the decomposition pathways of these three analogs to differ. All three compounds (thiophene, furan and pyrrole) are well-known to be more reactive for electrophilic reactions at the alpha-position with relative reactivity: pyrrole > furan > thiophene [90]. The lower onset of decomposition for pyrrole, as well as the presence of C_3 species following the decomposition of furan *vs* the C_4 species observed for thiophene, indicate their reactivity on Pd(111) to be consistent with this trend. However, it appears that pyrrole decomposition is considerably different than that for either of the two other analogs. Moreover, the formation of CO and (H)CN is more favorable than the formation of CS, as is evident by the reaction products observed in this study for each system. Also, from TPR data it has been shown that a sulfur overlayer is considerably more stable than an oxygen or nitrogen overlayer; O_2, formed from the recombination of atomic oxygen, desorbs from Pd(111) around 800 K [91,92] and, likewise, adsorbed N atoms have been observed to recombine and desorb as N_2 around 670 K from the same surface [93]. On a S-covered surface, however, temperatures greater than 1100 K have been reached without any signal for S_2 ever being reported [94–96], therefore, it is perhaps not surprising that S remains on the surface following decomposition, whereas O and N do not. This strong Pd—S bond would not, however, necessarily indicate that Pd promotion of desulfurization catalysts would suffer from rapid deactivation. The heat of formation of palladium sulfide is comparable to that of cobalt and nickel sulfides, the two metals most often employed as promoters for these catalysts. Moreover, as mentioned previously, PdS has been shown to catalyze HDS more efficiently (by more than an order of magnitude) than sulfides of Co and Ni.

LITD is a highly surface-sensitive technique which rapidly heats a portion of the surface, accessing the high energy pathway leading to desorption. As a result, tightly bound surface species, that would otherwise decompose under slow-heating conditions, desorb from the surface intact upon laser heating. Detection of reaction intermediates and stable species present in low concentrations, such as 1,3-butadiene and benzene which were not observed in TDS, is only possible with a technique having the sensitivity and characteristics of LITD. In addition, the capability provided by FTMS of monitoring all masses from

m/z 10 to 650 simultaneously eliminates the need for predetermining which masses to observe. Without this technique, unexpected reaction products (i.e. benzene from furan) may also go undetected.

These results suggest that Pd is selective for desulfurization and, hence, may enhance activity as a promoter on common HDS catalysts. Removal of oxygen and nitrogen is also facilitated, since CO and HCN desorb. All processes leave carbon on the surface, implying that the addition of hydrogen to the feed may be necessary to maintain catalyst acitivty.

Acknowledgements—The authors thank the Donors of The Petroleum Research Fund, administered by the American Chemical Society, for the partial support of this research. T.E.C. also thanks the Committee on Research of UC Davis for a Graduate Research Award and the Patricia Roberts Harris Foundation for a Graduate Fellowship Award. The authors also acknowledge I. M. Abdelrehim for his efforts in helping to acquire the data on thiophene and furan.

REFERENCES

1. Bond, G. C., *Heterogeneous Catalysis, Principles and Applications*, 2nd edn. Oxford University Press, Oxford, 1987.
2. Speight, J. G., *The Desulfurization of Heavy Oils and Residua*, Vol. 4. Marcel Dekker, Inc., New York, 1981.
3. Rollmann, L. D., *J. Catal.*, 1977, **46,** 243.
4. Drushel, H. V., *American Chemical Society Preprint; Division of Petroleum Chemistry*, 1970, **15,** C13.
5. Richter, F. P., Williams, A. L. and Meisel, S. L., *J. Am. Chem. Soc.*, 1956, **78,** 2166.
6. Cadey, W. E. and Seelig, H. S., *Ind. Eng. Chem.*, 1952, **44,** 2636.
7. Furimsky, E., *Catal. Rev. Sci. Eng.*, 1983, **25,** 421.
8. Katzer, J. R. and Sivasubramanian, R., *Catal. Rev.*, 1979, **20,** 155.
9. Odebunmi, E. O. and Ollis, D. F., *J. Catal.*, 1983, **80,** 76.
10. Wallace, S., Barthe, K. D. and Perry D. L., *Fuel*, 1989, **68,** 1450.
11. Sarbak, Z., *Acta Chim. Hung.*, 1990, **127,** 371.
12. Chary, K. V. R., Rao, K. S. R., Muralidhar, G. and Rao, P. K., *Carbon*, 1991, **29,** 478.
13. Zaera, F., Kollin, E. B. and Gland, J. L., *Langmuir*, 1987, **3,** 555.
14. Stöhr, J., Gland, J. L., Kollin, E. B., Koestner, R. J., Muetterties, E. L. and Sette, F., *Phys. Rev. Lett.*, 1984, **53,** 2161.
15. Zaera, F., Gland, J. L. and Kollin, E. B., *Surf. Sci.*, 1987, **184,** 75.
16. Heise, W. H. and Tatarchuk, B. J., *Surf. Sci.*, 1989, **207,** 297.
17. Cocco, R. A. and Tatarchuk, B. J., *Surf. Sci.*, 1989, **218,** 127.
18. Gellman, A. J., Neiman, D. and Somorjai, G. A., *J. Catal.*, 1987, **107,** 92.
19. Sexton, B. A., *Surf. Sci.*, 1985, **163,** 99.
20. Solomon, J. L., Madix, R. J. and Stöhr, J., *J. Chem. Phys.*, 1990, **94,** 4012.
21. Crew, W. W. and Madix, R. J., *J. Am. Chem. Soc.*, 1993, **115,** 729.
22. Schoofs, G. R. and Benziger, J. B., *Surf. Sci.*, 1987, **192,** 373.
23. Netzer, F. P., Bertel, E. and Goldmann, A., *Surf. Sci.*, 1988, **199,** 87.
24. Henry, R. M., Walker, B. W. and Stair, P. C., *Surf. Sci.*, 1985, **155,** 732.
25. Tourillon, G., Raaen, S., Skotheim, T. A., Sagurton, M., Garrett, R. and Williams, G. P., *Surf. Sci.*, 1987, 184.
26. Pan, F. M., Stair, P. C. and Fleisch, T. H., *Surf. Sci.*, 1986, **177,** 1.
27. Land, D. P., Pettiette-Hall, C. L., Hemminger, J. C. and McIver, R. T., Jr., *Accts Chem. Res.*, 1991, **24,** 42.
28. Land, D. P., Pettiette-Hall, C. L., McIver, R. T., Jr. and Hemminger, J. C., *J. Am. Chem. Soc.*, 1989, **111,** 5970.
29. Hall, R. B. and Bares, S. J., in *Chemistry and Structure at Interfaces: New Optical Probes*, ed. R. B. Hall and A. B. Ellis. VCH, Deerfield Beach, FL, 1986, p. 85.
30. George, S. M., in *Investigations of Surfaces and Interfaces—Part A*, Vol. 1XA, 2nd end., ed. B. W. Rossiter and R. C. Baetzold. John Wiley & Sons, New York, 1993, p. 453.
31. Cowin, J. P., Auerbach, D. J., Becker, C. and Wharton, L., *Surf. Sci.*, 1978, **78,** 545.
32. George, S. M., Desantolo, A. M. and Hall, R. B., *Surf. Sci.*, 1985, **159,** L425.
33. Gross, M. L. and Rempel, D. L., *Science*, 1984, **226,** 261.
34. Wilkins, C. L., Chowdhury, A. K., Nuwaysir, L. M. and Coates, M. L., *Mass Spectrum. Rev.*, 1989, **8,** 67.
35. Russell, D. H., *Mass Sepctrom. Rev.*, 1986, **5,** 167.
36. Marshall, A. G., *Accts. Chem. Res.*, 1985, **18,** 316.
37. Land, D. P., Pettiette-Hall, C. L., Sander, D., McIver, R. T., Jr. and Hemminger, J. C., *Rev. Sci. Instr.*, 1990, **61,** 1674.
38. Land, D. P., Abdelrehim, I. M., Thornburg, N. A. and Sloan, J. T., *Anal. Chim. Acta*, 1995, **307,** 321.
39. Bartmess, J. E. and Georgiadis, R. M., *Vacuum*, 1983, **33,** 149.
40. Dannetun, H., Lundström, I. and Peterson, L.-G., *Appl. Surf. Sci.*, 1987, **29,** 361.
41. *The Wiley/NBS Registry of Mass Spectral Data*, vol. 1, ed. F. M. McLafferty and D. Stauffer. John Wiley & Sons, New York, 1989.
42. Caldwell, T. E. and Land, D. P., in preparation.
43. Lipsch, J. M. J. G. and Schuit, G. C. A., *J. Catal.*, 1969, **15,** 179.
44. Conrad, H., Ertl, G., Koch, J. and Latta, E. E., *Surf. Sci.*, 1974, **43,** 462.
45. Caldwell, T. E., Abdelrehim, I. M. and Land, D. P., *J. Am. Chem. Soc.*, 1996, **118,** 907.
46. Rucker, T. G., Logan, M. A., Gentle, T. M., Muetterties, E. L. and Somorjai, G. A., *J. Phys. Chem.*, 1986, **90,** 2703.
47. Patterson, C. H. and Lambert, R. M., *J. Am. Chem. Soc.*, 1988, **110,** 6871.
48. Patterson, C. H., Mundenar, J. M., Timbrell, P. Y., Gellman, A. J. and Lambert, R. M., *Surf. Sci.*, 1989, **208,** 93.

49. Abdelrehim, I. M., Thornburg, N. A., Sloan, J. T. and Land, D. P., *Surf. Sci.*, 1993, **298,** L169.
50. Pacchioni, G. and Lambert, R. M., *Surf. Sci.*, 1994, **304,** 208.
51. Abdelrehim, I. M., Thornburg, N. A., Sloan, J. T., Caldwell, T. E. and Land, D. P., *J. Am. Chem. Soc.*, 1995, **117,** 9509.
52. Abdelrehim, I. M., Caldwell, T. E. and Land, D. P., *J. Phys. Chem.*, 1996, **100,** 10265.
53. Sherman, M. G., Land, D. P., Hemminger, J. C. and McIver, R. T., Jr., *Chem. Phys. Lett.*, 1987, **137,** 298.
54. Baumgartner, K. M., Volmer-Uebing, M., Toborski, J., Bauelrle, P. and Umbach, E., *Ber. Bunsenges. Phys. Chem.*, 1991, **95,** 1488.
55. Schoofs, G. R., Preston, R. E. and Benziger, J. B., *Langmuir*, 1985, **1,** 313.
56. Lang, J. R. and Masel, R. I., *Surf. Sci.*, 1987, **183,** 44.
57. Kelly, D. G., Salmeron, M. and Somorjai, G. A., *Surf. Sci.*, 1986, **175,** 465.
58. Gellman, A. J., Farias, M. H., Salmeron, M. and Somorjai, G. A., *Surf. Sci.*, 1984, **136,** 217.
59. Roberts, J. T. and Friend, C. M., *Surf. Sci.*, 1987, **186,** 201.
60. Kelly, D. G., Odriozola, J. A. and Somorjai, G. A., *J. Phys. Chem.*, 1987, **91,** 5695.
61. Piancastelli, M. N., *Solid State Commun.*, 1987, **63,** 85.
62. Furimsky, E., *A. I. Ch. E. J.*, 1979, **25,** 306.
63. Furimsky, E., *Catal. Rev. Sci. Eng.*, 1980, **22,** 371.
64. Bussell, M. E. and Somorjai, G. A., *Cat. Lett.*, 1989, **3,** 1.
65. Ratnasany, P. and Sivasanker, S., *Catal. Rev. Sci. Eng.*, 1980, **22,** 410.
66. Chianelli, R. R., in *Catalysis and Surface Science*, ed. H. H. a. G. A. Somorjai. Marcel Dekker, Inc., New York, 1985, p. 61.
67. Tinseth, G. R. and Watson, P. R., *J. Am. Chem. Soc.*, 1991, **113,** 8549.
68. Patterson, C. H. and Lambert, R. M., *J. Phys. Chem.*, 1988, **92,** 1266.
69. Caldwell, T. E., Abdelrehim, I. M. and Land, D. P., *Surf. Sci.*, 1996, **367,** L26.
70. Ormerod, R. M. and Lambert, R. M., *Cat. Lett.*, 1990, **6,** 121.
71. Ormerod, R. M., Baddeley, C. J., Hardacre, C. and Lambert, R. M., *Surf. Sci.*, 1996, **360,** 1.
72. Zaera, F., *J. Phys. Chem.*, 1990, **94,** 5090.
73. Paul, A. and Bent, B. E., *J. Catal.*, 1994, **147,** 264.
74. Ali, A.-K. M., Saleh, J. M. and Hikamat, N. A., *J. Chem. Soc., Faraday Trans.*, 1987, **83,** 2391.
75. Zhou, Y., Henderson, M. A., Feng, W. M. and White, J. M., *Surf. Sci.*, 1989, **224,** 386.
76. Solymosi, F., Kiss, J. and Revesz, K., *J. Phys. Chem.*, 1991, **94,** 8510.
77. Beanan, L. R. and Keister, J. B., *Organometallics*, 1985, **4,** 1713.
78. Churchill, M. R., Buttrey, L. A., Keister, J. B., Ziller, J. W., Janik, T. S. and Striejewske, W. S., *Organometallics*, 1990, **9,** 766.
79. Keister, J. B., Personal letter proposing collaboration of IR studies of the C3H3 species on Pd(111). *Private Communication*, 1996.
80. Ormerod, R. M., Ph.D. Dissertation, Cambridge, 1989.
81. Patzer, J. F. and Montagna, A. A., *Ind. Eng. Chem., Process Des. Dev.*, 1980, **19,** 382.
82. Kordesch, M. E., Stenzel, W. and Conrad, H., *Surf. Sci.*, 1988, **205,** 100.
83. Gdowski, G. E., Felter, T. E. and Stulen, R. H., *Surf. Sci.*, 1987, **181,** L147.
84. Wang, L. P., Tysoe, W. T., Ormerod, R. M., Lambert, R. M., Hoffman, H. and Zaera, F., *J. Phys. Chem.*, 1990, **94,** 4236.
85. Bertolo, M. and Jacobi, K., *Surf. Sci.*, 1992, **265,** 1.
86. Kordesch, M. E., Stenzel, W. and Conrad, H., *J. Electron Spectrosc. Rel. Phen.*, 1986, **39,** 89.
87. Smith, G. V., Hinckley, C. C. and Behbahany, F., *J. Catal.*, 1973, **30,** 218.
88. Duben, A. J., *J. Phys. Chem.*, 1978, **82,** 348.
89. Kwart, H., Schuit, G. G. A. and Gates, B. C., *J. Catal.*, 1980, **61,** 128.
90. Streitwieser, A., Jr and Heathcock, C. H., *Introduction to Organic Chemistry*, 2nd edn. Macmillan Publishing Company, New York, 1981, p. 1069.
91. Matsushima, T., *Surf. Sci.*, 1985, **157,** 297.
92. Guo, X., Hoffman, A. and Yates, J. T., *J. Chem. Phys.*, 1989, **90,** 5787.
93. Conrad, H., Ertl, G., Kuppers, J. and Latta, E. E., *Surf. Sci.*, 1977, **65,** 245.
94. Gellman, A. J., *J. Phys. Chem.*, 1992, **96,** 790.
95. Gellman, A. J., *J. Am. Chem. Soc.*, 1991, **113,** 4435.
96. Gellman, A. J., *Langmuir*, 1991, **7,** 827.